

Poly(lactic-co-glycolic acid) microspheres added to fixative cements and its role on bone infected architecture

Blanca Ibarra,^{1,2†} Joaquin García-García,^{3†} Galo Azuara,^{4†} Blanca Vázquez-Lasa,² Miguel A. Ortega,^{1,2} Ángel Asúnsolo,^{5,7} Julio San Román,² Julia Buján,^{1,2,7} Natalio García-Honduvilla,^{1,2,7‡} Basilio De la Torre^{6,7‡}

¹Departments of Medicine and Medical Specialities, Faculty of Medicine and Health Sciences, University of Alcalá, Alcalá de Henares, Madrid, Spain

²Networking Biomedical Research Center on Bioengineering, Biomaterials and Nanomedicine (CIBER-BBN), Institute of Polymer Science and Technology (ICTP-CSIC), Madrid, Spain

³Service of Orthopedic Surgery of University Hospital Principe de Asturias, Madrid, Spain

⁴Service of Traumatology of University Hospital of Guadalajara, Madrid, Spain

⁵Department of Surgery, Medical and Social Sciences, Faculty of Medicine and Health Sciences, University of Alcalá, Alcalá de Henares, Madrid, Spain

⁶Service of Traumatology of University Hospital Ramón y Cajal, Madrid, Spain

⁷Ramón y Cajal Institute of Sanitary Research (IRYCIS), Madrid, Spain

Received 27 December 2017; revised 24 September 2018; accepted 26 January 2019

Published online 19 February 2019 in Wiley Online Library (wileyonlinelibrary.com). DOI: 10.1002/jbm.b.34342

Abstract: Joint prostheses are an essential element to improve quality of life. However, prostheses may fail due to several factors, including the most frequent cause, *Staphylococcus aureus* infection. The identification of new fixing bone cements with less reactivity on bone tissue and an adequate response to infection remains a primary challenge. The aim of this study is to evaluate the response of bone tissue in rabbits after introduction of a hydroxyapatite-coated titanium rod with a commercial fixative cement (Palacos[®]) compared to a modified experimental cement (EC) containing poly(lactic-co-glycolic acid) (PLGA) microspheres in the presence or absence of contaminating germs. This study used 20 New Zealand rabbits which were divided into four groups ($n = 5$) depending on the presence or absence of *S. aureus* and the use of

commercial (Palacos[®]) or EC. A histological method, based on bone architecture damage, was proposed to evaluate from 1 to 9 the histological results and the response of the infected tissue. The macrophage response was also evaluated using monoclonal antibody RAM-11. The study showed better bone conservation with the use of EC with PLGA microspheres against the Palacos[®] commercial cement, including the non-contaminated and contaminated groups. © 2019 The Authors. *Journal of Biomedical Materials Research Part B: Applied Biomaterials* published by Wiley Periodicals, Inc. *J Biomed Mater Res Part B: Appl Biomater* 107B:2517–2526, 2019.

Key Words: regenerative medicine, osteomyelitis, biomaterials, PLGA microspheres, macrophagic response

How to cite this article: Ibarra B, García-García J, Azuara G, Vázquez-Lasa B, Ortega MA, Asúnsolo Á, San Román J, Buján J, García-Honduvilla N, De la Torre B. 2019. Poly(lactic-co-glycolic acid) microspheres added to fixative cements and its role on bone infected architecture. *J Biomed Mater Res Part B* 2019;107B:2517–2526.

INTRODUCTION

The frequency of primary or revision hip and knee arthroplasty has exponentially increased in recent years. The prevalence rates of hip arthroplasty and knee arthroplasty were 0.83% and 1.52%, respectively, in the United States in 2010.¹ The estimated incidence in 2020 will be 75% in hip (prevalence 1.45%) and 110% in knee arthroplasty (prevalence 3.20%).² The number of primary knee arthroplasties was 88,038 (1.5 per 1000 inhabitants) and 79,949 (1.28 per 1000

inhabitants) in primary hip arthroplasties in the United Kingdom in 2012.³ Primary hip arthroplasty rates in Spain in 2005 were 4.3 per 10,000 inhabitants and knee arthroplasty rates were 7.3 per 10,000 inhabitants.⁴

Between 30% and 50% of arthroplasties fail in the first 10 years, with most failures occurring in the first 2 years.⁵ Infection and aseptic loosening, hip instability, and periprosthetic fracture are the most important causes of failure. The prevalence of infection in 2003 was ~1.3% in primary

[†]These authors contributed equally to this work.

[‡]These authors shared senior authorship in this work.

Correspondence to: J. Buján; e-mail: mjulia.bujan@uah.es

Contract grant sponsor: SECOT (Spanish Society of Orthopedic Surgery and Traumatology); contract grant number: 2016/0055

Contract grant sponsor: MINECO (Spanish Ministry of Economy and Competitiveness); contract grant numbers: MAT2014-51918-C2-1-R, MAT-201784277-R

Contract grant sponsor: MITIC-CM (Community of Madrid); contract grant number: B2017/BMD-3804

arthroplasty and between 2% and 20% in revision surgery. Estimations for the year 2030 suggest an increase in infection rates up to 6.5% in hip and 6.8% in knee in the USA⁶ based on the aging of the population and increased obesity.⁷ Similar estimations are found in Europe.³

Staphylococci (*Staphylococcus aureus* and *Staphylococcus epidermidis*) represent 65%–75% of cases related with prosthetic infection.^{8,9} These germs develop a biofilm around the implant that hinders infection diagnosis and the efficacy of antibiotic treatment.¹⁰

The infection affects tissues and the capacity for remodeling, which are difficult issues to assess in clinical practice. Experimental models are necessary to investigate these issues. Several groups developed improved new experimental models of osteomyelitis caused by *S. aureus* and varied the bacterial strain, the inoculum concentration, and the subsequent investigative methods.¹¹ Therefore, clinical, microbiological, or radiological evaluation is constant between studies,^{12,13} but the histological methods vary widely depending on the researchers. Scales created by authors, such as Smeltzer¹⁴ or Petty,¹⁵ and the multiple adaptations or variations of these scales,¹⁶ are widely used, but both scales evaluate very specific aspects of bone histoarchitecture. Therefore, these scales exhibit high variability depending on the bacterial strain, inoculum, and the selected animal model.

Bone cement spacers reduce the rate of infection of prosthetic spares and maintain a higher concentration of local antibiotic in the affected area compared to oral treatments. Some of the most common commercial bone cements are Palacos R[®] or Simplex[®], and better results are obtained with the Palacos R[®].^{17,18} Several attempts to modify the formulation of some of these commercial cements were reported recently via the introduction of soluble components into the solid phase of the cement. This change increased the porosity of the product and facilitated the subsequent release of the antibiotics over a longer period of time.^{19,20}

The aim of this study was focused for improving some of the current commercial cements, and we obtained promising results in *in vitro* studies.²¹ Therefore, this study evaluated modified cement in an experimental model of osteomyelitis and investigated the affected tissues using a new method of histological staging.

MATERIALS AND METHODS

This study used 20 New Zealand rabbits (weight range of 2.5–3 kg). Animals were managed in accordance with the current International Regulations on Experimental Animals (609/86/EEC and ETS 123) at the Animal Research Center of the University of Alcalá. The study protocol received approval from the Committee on the Ethics of Animal Experiments of the University of Alcalá (CEI UAH 2011017). The diet of the animals was available *ad libitum*.

A strain of *S. aureus* (generously provided by the University Hospital of Guadalajara, Spain, Identification Code 07041246773271) was prepared in a tube suspension with 3 mL of saline and a germ inoculum adjusted to 4 mL, following the McFarland scale (BioMérieux, Marcy l'Etoile, France),

equivalent to 1.2×10^9 CFU/mL. A titanium rod coated with hydroxyapatite was introduced for 24 h in each tube with this suspension to produce contamination. Scanning electron microscopy (SEM) revealed the presence of germs adhered to the rod after removal from the suspension (Fig. 1). This rod was the contaminated implant that was introduced into the bone tissue.

We used Palacos R[®] (Heraeus Medical, Germany) as the commercial cement (CC) following the composition of previous studies,²¹ and we performed a partial replacement of the solid phase of Palacos R[®] with poly(lactic-co-glycolic acid) (PLGA) microspheres (45%) as the experimental cement (EC). The animals were divided into four groups ($n = 5$) depending on the presence or absence of germ in the implant and the use of commercial or EC. Table I shows the name and composition of each group.

The anesthetic protocol consisted of intramuscular administration of ketamine hydrochloride (Ketolar[®], 70 mg/kg), diazepam (Valium[®], 1.5 mg/kg), and chlorpromazine (Largactil[®] 1.5 mg/kg). A coetaneous incision was made in the distal femur until we reached 2.5–3 cm. The condyle was exposed, and an orifice was created manually in the metaphysis region until the medullar canal was reached. The rod was introduced into the bone orifice, and the bone cement (solid phase and liquid phase mixture) was prepared. The mixture acquired a pasty consistency, and the bone cement was introduced until the hole was completely plugged. A thorough cleaning was performed during the setting of the cement, and the wound was closed.

Animals were sacrificed after 3 weeks. Samples were introduced into a fixative and decalcifying solution (Osteosoft[®]) for 60 days. Samples were processed for histological study, including embedding in paraffin, slicing at a thickness of 5 μ m, and staining for histological study using hematoxylin–eosin and Gram stains. Immunohistochemistry was performed using the monoclonal antibody RAM-11 (DakoCytomation, Glostrup, Denmark) to quantitatively analyze the macrophage tissue response.

A scale was developed to assess the degree of bone destruction and quantify the histological result. This gradation included values between 1 and 9 that globally evaluated the bone response to the aggression and its remodeling. Table II shows the degree of destruction classification.

Five samples per rabbit were stained with hematoxylin–eosin, and two independent observers blindly graded the samples. A final mean per rabbit and group was generated for later statistical analysis. The macrophage response was quantified using immunohistochemistry with RAM-11 in a total of 15 fields (20 \times) per animal in each group.

The results were analyzed using STATA version 14 (Stata Corp, TX). One mean per group and the mean deviation of each group were generated. Nonparametric tests (Mann–Whitney *U* test) were used to evaluate the role of infection in bone destruction, the behavior of both types of cements in the presence of infection, and the behavior of EC independently of the presence or absence of infection. The level of statistical significance was set at $p \leq 0.05$. Graphical representations of the data were performed using STATA version 14 and GraphPad Prism 7 (GraphPad, San Diego, CA).

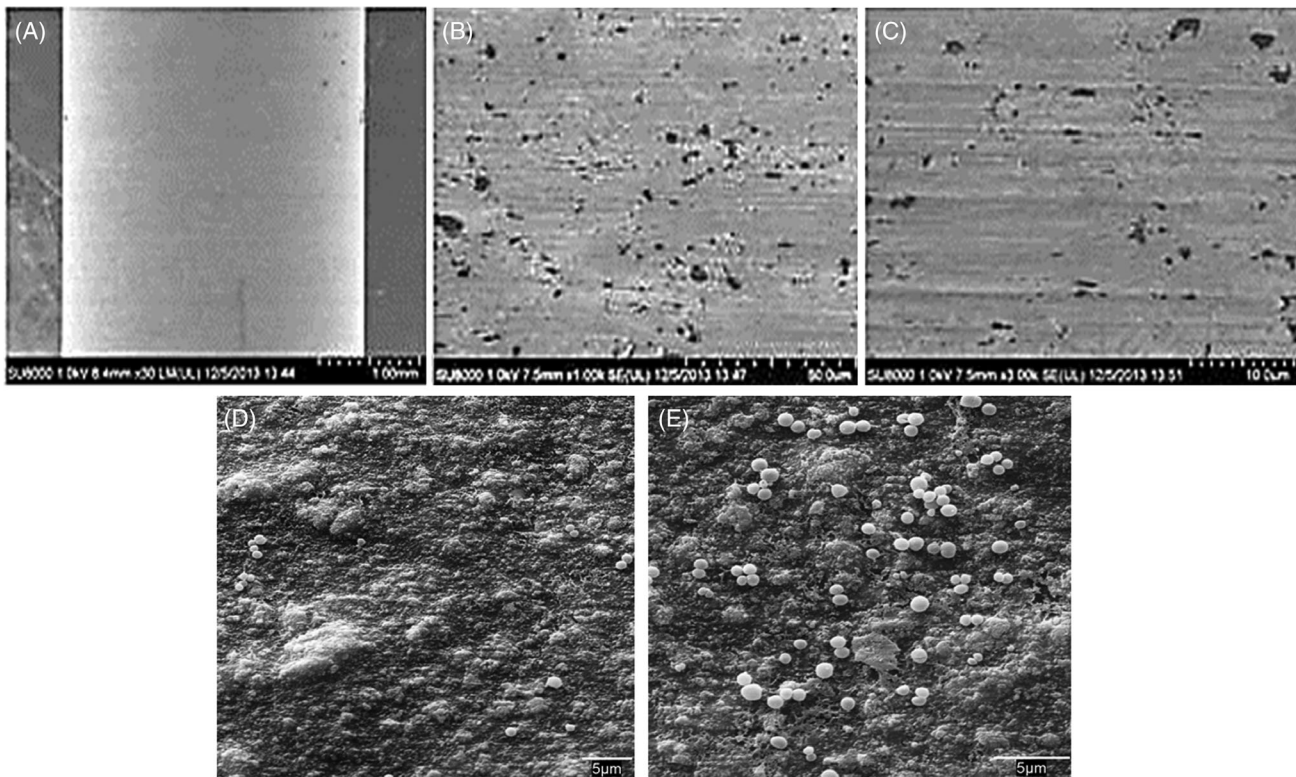


FIGURE 1. A–C: SEM images show the titanium sterile rod coated with HA. D,E: Titanium rod contaminated with *S. aureus*.

RESULTS

Histological staging model

This model was designed to study the histoarchitecture alterations after injury (sterile rod) with commercial or ECs, in the presence or absence of *S. aureus*. We are conscious about the limitations of this type of study to be used as a clinical method for diagnosis. This design revealed the bacterial effects on bone structures with a global view. A detailed histological scale was created using the parameters in Table II to describe the structures in this model that were representative of the area to be studied, including the epiphysis, epiphyseal cartilage, and metaphyseal zone, and show the ascending degree of destruction of the structures involved (Fig. 2).

The implant in animals without infection (groups 1 and 2)

Animals with a sterile rod implant and Palacos R[®] (group 1) exhibited a good metaphyseal repair response. Implant encapsulation surrounded by new bone formation in which the cement remained was observed in all animals. The metaphyseal cartilage was partially unstructured, but it was well preserved and delimited the epiphyseal cavity, in which

TABLE I. Name and Composition for Each Group of Study

Group	Rod	Cement
1	Sterile	Palacos R [®]
2	Sterile	Palacos R [®] + PLGA
3	Contaminated	Palacos R [®]
4	Contaminated	Palacos R [®] + PLGA

moderate trabecular disruption was observed in the path of the rod implant [Fig. 3(A)].

Animals with a sterile rod implant and Palacos R[®] + PLGA (group 2) revealed the presence of the imprints from the rod, and great bone remodeling around the implant area, which emphasized a higher density of metaphyseal bone (Fig. 4). A highly conserved metaphyseal cartilage and great recovery of spongy bone on the path of the rod implant were also observed [Fig. 3(B)].

The implant in animals with infection (groups 3 and 4)

Animals with a contaminated rod implant and commercial cement (Palacos R[®]), group 3, exhibited an important alteration that did not allow conservation of the histoarchitecture in the studied area. A loss of integrity of the bone structure was observed in the histological images of necrosis and

TABLE II. Degree of Destruction Scheme

Degree of destruction	Degree	Criteria
Light destruction	From 1 to 3	Destruction affects only the bone closest to the insertion of the rod.
Moderate destruction	From 4 to 6	The area of insertion of the rod and part of the near cartilage is affected.
Severe destruction	From 7 to 9	Global destruction of the bone, overcoming the adjacent cartilage.

The bone disruption is graded in light (from 1 to 3), moderate (from 4 to 6), and severe (from 7 to 9).


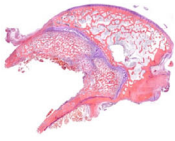
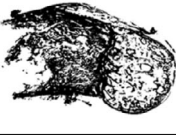
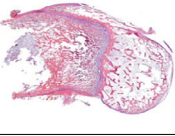

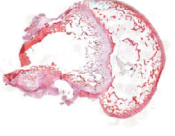


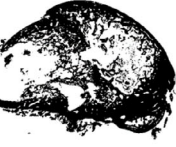
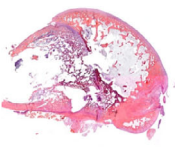




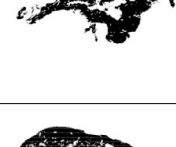

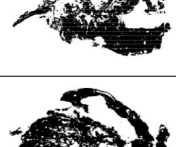
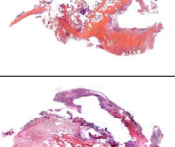
GRADE	CHARACTERISTICS	SCHEME AND REPRESENTATIVE EXAMPLE	
1	Minimum disruption. Cartilage intact. The bone is restructured with well-organized new bone around the defect.		
2	Very slight disruption. Cartilage intact. Small disruption of bone around the defect.		
3	Mild disruption. Cartilage intact. There is a greater degree of disruption in bone structure around the defect, which does not exceed cartilage.		
4	Moderate disruption. The bone trabeculae surrounding the defect are lower. The cartilage is disrupted in the area closest to the defect and loses its uniformity.		
5	Moderate disruption. Lower density of bone trabeculae around the defect with partial loss of cartilage, without suffering a total loss or the bone farthest from the defect.		
6	Moderate disruption. Absence in the formation of bone trabeculae or presence of them in a disorganized way around the defect. Total loss of articular cartilage, being able to slightly disrupt the furthest bone from the defect.		
7	Severe disruption. Absence in the formation of bone trabeculae around the defect. Total loss of articular cartilage, moderately destructuring the bone trabeculae furthest from the defect.		
8	Severe disruption. Severe overall bone disorganization, with absence of articular cartilage and presence of very disorganized bone tissue.		
9	Severe disruption. There is no clear organization of bone tissue.		

FIGURE 2. Detailed histological scale to describe the structures in this model study. The figure shows a detailed description, a black and white scheme, and a final representative panoramic view of each parameter.

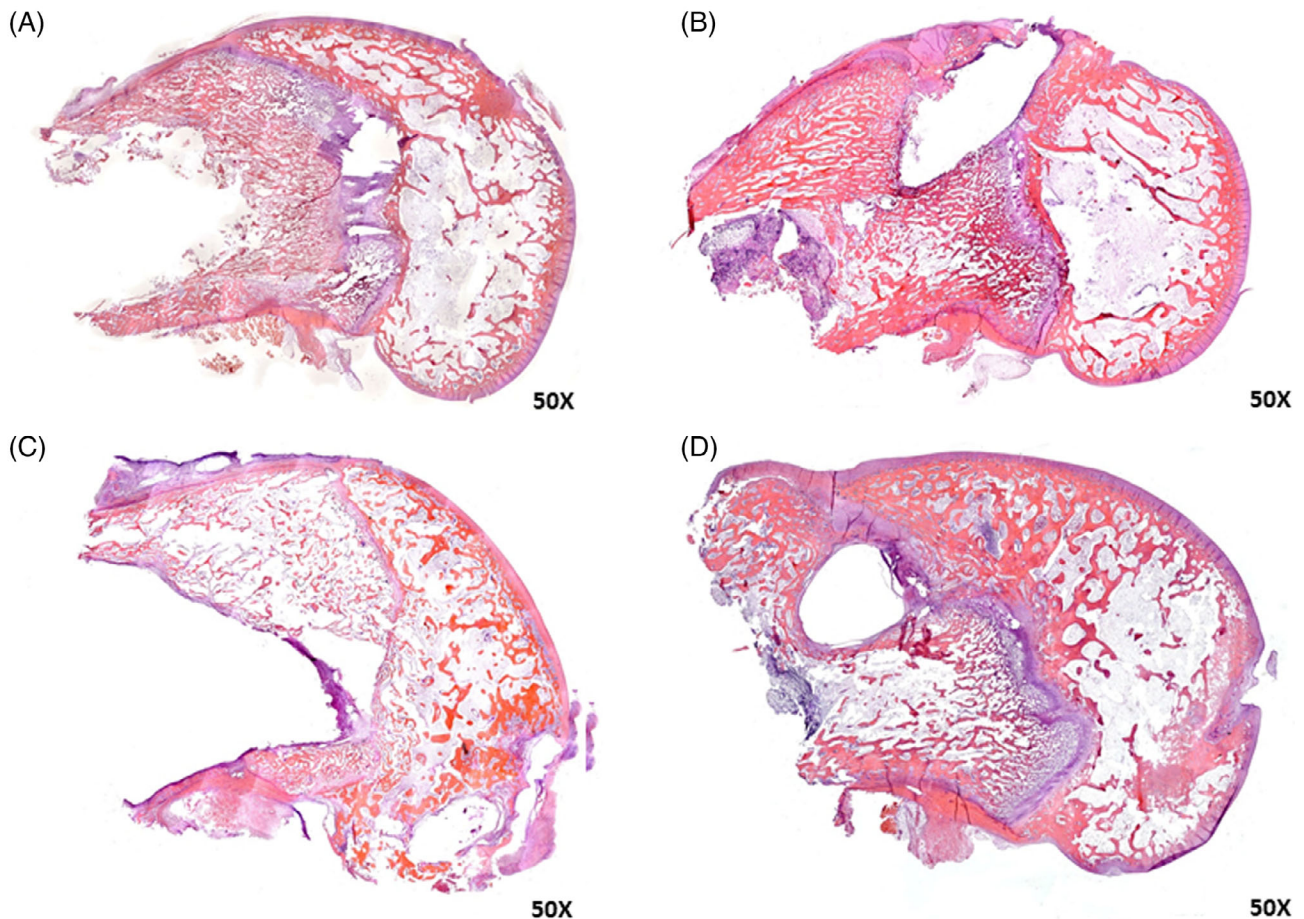


FIGURE 3. Panoramic views. A: Sterile rod + Palacos[®] (50×). B: Sterile rod + Palacos[®] + PLGA (50×). C: Contaminated rod + Palacos[®] (50×). D: Contaminated rod + Palacos[®] + PLGA (50×).

scattered tissue remains. There were no signs of tissue repair in the implant or surrounding areas. The epiphysis exhibited a highly unstructured appearance. The metaphyseal cartilage was heavily damaged or absent in some areas, and the remains of the implanted cement remained in contact with the surrounding tissue [Fig. 3(C)].

Animals with the contaminated rod implant and EC (Palacos R[®] + PLGA), group 4, showed an excellent response to the aggression. The rod implant was surrounded by a capsule in which new bone was detected, and the cemented remains were attached. Very good preservation of the tissue histoarchitecture, a well-preserved metaphyseal cartilage, and an absence of epiphyseal destruction were observed, and only the presence of newly formed bone and fibrosis along the path of the rod were observed [Fig. 3(D)].

Statistical analysis

The disruption degree obtained in animals with no infection was low (mean 1.5 IQR [1–3]). The EC (Palacos R[®] + PLGA) maintained this low degree of disruption while the commercial cement (Palacos R[®]) increased extraordinarily in the animals with a contaminated rod ($p = 0.042$). Global comparison of the study groups revealed that group 4 (contaminated rod + Palacos R[®] + PLGA) maintained the characteristics of

preservation, histological structure, and degree of disruption similar to group 2 (sterile rod + Palacos R[®] + PLGA), despite the infected. Figure 5 shows the comparative histograms of each of the study groups. These differences are consistent with the results observed histologically.

Study of the infection

The contaminated rods exhibited the presence of *S. aureus* on the hydroxyapatite coating (Fig. 1). The presence of bacterial infection 3 weeks later was confirmed using the Gram staining technique. The presence of infection in animals in which the contaminated rod was fixed with Palacos R[®] cement (group 3) was difficult to assess because of the severe degree of disruption of the affected area. The presence of bacteria in other areas was shown as colonies located in bone and cartilage. The bacterial presence was contained around the cement when the cement included Palacos R[®] + PLGA (group 4), and colonization was observed only in adjacent areas [Fig. 6(A)]. We observed the presence of bacterial colonies in the metaphysis, cartilage, and trabecular bone [Fig. 6(B,C)]. The presence of infection in this group appeared higher, but this observation was due to the severe degree of destruction in group 3 (Palacos R[®]) with the loss of tissue at the moment of histological processing.

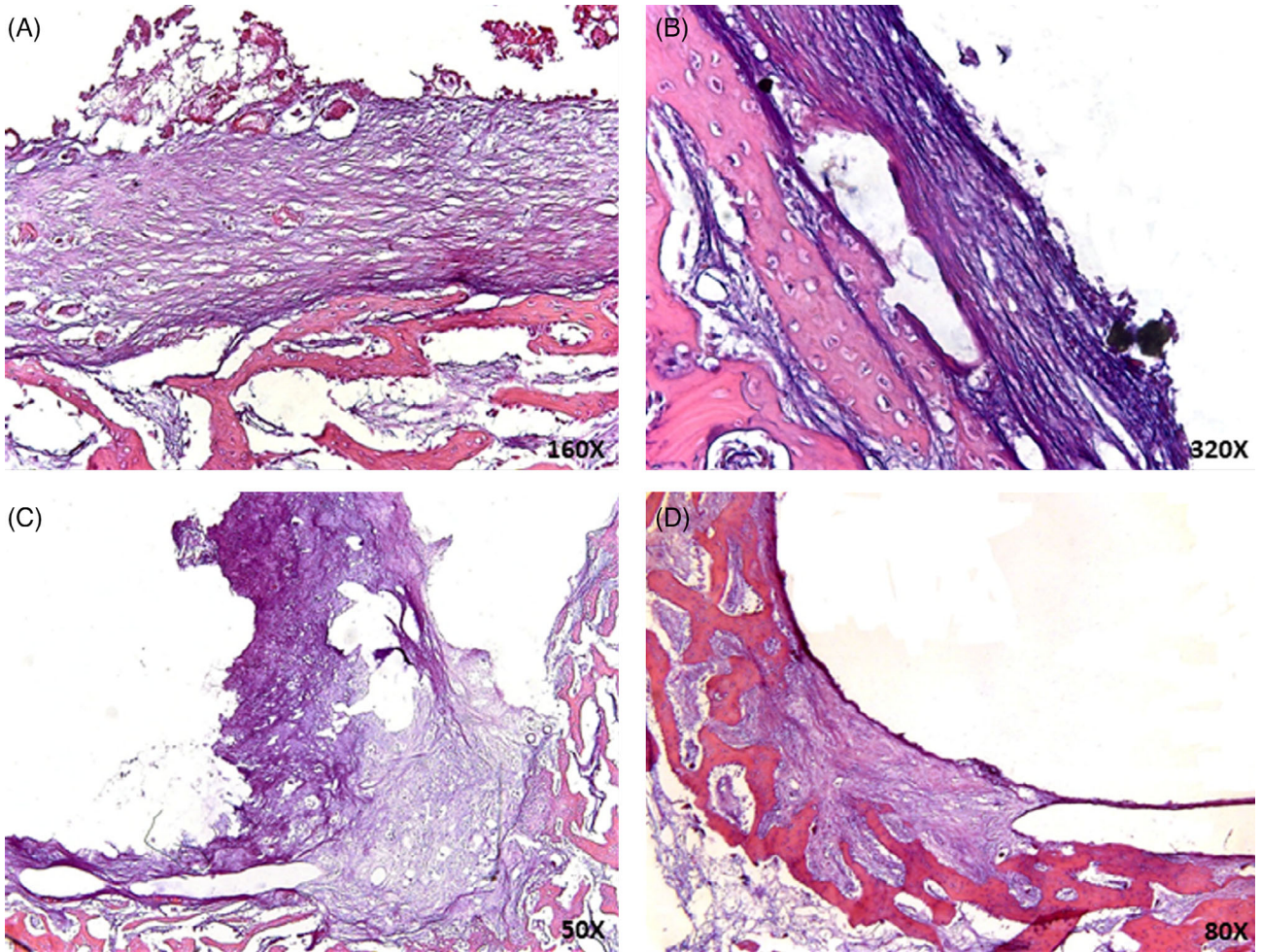


FIGURE 4. A: Sterile rod + Palacos[®] (160×). B: Sterile rod + Palacos[®] + PLGA (320×). C: Contaminated rod + Palacos[®] (50×). D: Contaminated rod + Palacos[®] + PLGA (80×).

Description and analysis of RAM-11

Immunohistochemistry with RAM-11 revealed a moderate macrophage reaction in the noninfected group with Palacos R[®] cement (group 1). Primary expression occurred in the

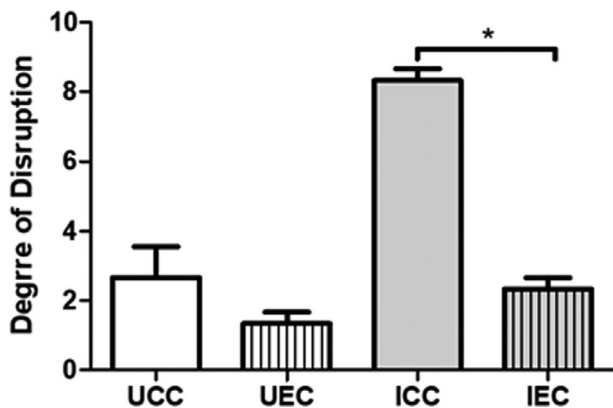


FIGURE 5. Histograms comparing the degree of disruption. The experimental cement (Palacos R[®] + PLGA) maintained this low degree of disruption while the commercial cement (Palacos R[®]) increased extraordinarily in the animals with a contaminated rod ($p = 0.042$). CC: Palacos R[®]; EC: Palacos R[®] + PLGA. * $p < 0.05$.

capsular tissue, next to areas with biomaterial remains, and the bone marrow surrounding the insertion of the rod. However, the noninfected group with Palacos R[®] + PLGA (group 2) exhibited bone tissue with a highly respected area, where the macrophage reaction was limited to the capsular zone generated by the biomaterial. The rest of the surrounding bone tissue contained some isolated macrophages [Fig. 7(A)].

The infected group with Palacos R (group 3) revealed an intense macrophage expression surrounding the defect, with the formation of large multinucleated giant cells around the damaged bone that followed the insertion path of the rod. Group 4 (Palacos R[®] + PLGA cement) exhibited a lower macrophage response in all animals [Fig. 7(B–D)].

The macrophage response in groups with no infection was significantly higher in group 1 than group 2 ($p < 0.01$). Samples with infection were not statistically significant different between cements, and an adequate macrophage response was observed in both groups (Fig. 8).

DISCUSSION

The introduction of PLGA microspheres to modify the commercial cement formulas, such as Palacos[®], controls the aggressiveness of tissue infection and exhibits a better

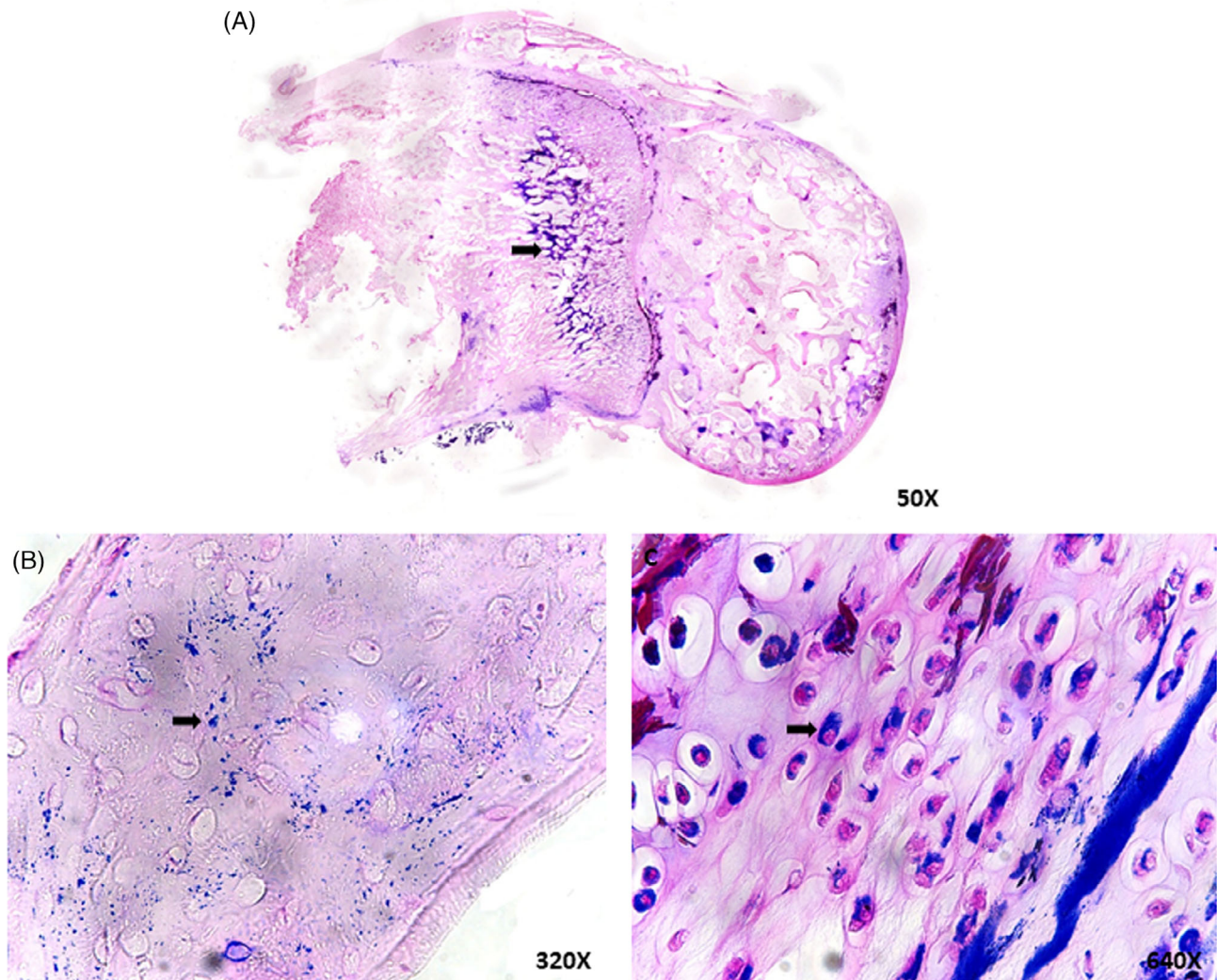


FIGURE 6. A: Panoramic view of Gram staining showing a contaminated rod + Palacos® + PLGA (50×). B: Gram staining detail showing a contaminated rod + Palacos® + PLGA (bone trabeculae) (320×). C: Gram staining detail showing a contaminated rod + Palacos® + PLGA (cartilage) (640×). Arrow indicates infected bone and cartilage cells.

preservation and remodeling of the architecture of the surrounding bone compared to Palacos® bone cement.

In vitro previous studies showed that modification of bone spacer cements with microspheres of PLGA or any other formulations improved the release of antibiotics to prevent infection and the ability to remodel a bone defect.^{21–24} These steps are the basis for future improvements in commercial bone spacer formulations, which will reduce the morbidity associated with these interventions in a medium term. Now we have observed that after *in vivo* implantation of sterile rods filled with this modified spacer cement, it induced significant positive response with an increase of bone neoformation around the implanted rod areas compared to commercial spacer cements without modification. It is possible that the presence of PLGA can induce certain osteoinductive capacity of Palacos® offering a different surface in contact to eroded bone.

Prosthetic infection is one of the most demanding complications after total or partial arthroplasty. Diagnosis of infection

remains an important challenge, and it relies on different parameters.

The priority in this scenario is to determine the possible infection and establish an appropriate treatment. Some authors used synovial biopsy to correctly diagnose the germ, but the methodologies varied, and inconsistent results were obtained.^{25–31} Biopsies of the periprosthetic tissue from the space between the prosthesis and the bone were also published.³² The authors describe a sensitivity of 88%. Martinez-Perez et al.³³ showed the importance of the clinical strains compared to the collection strain. Clinical strains exhibited a higher adherence at low concentrations compared to the collection strains. Clinical strains exhibited a capacity for cell destruction at high concentrations. In this sense, we used a clinical strain to contaminate the sterile rods. This effect may be relevant in our model in which the tissue destruction was the more evident observed characteristic.

Li et al.³⁴ studied bone architecture and remodeling after implantation of a prosthesis using computerized micrography

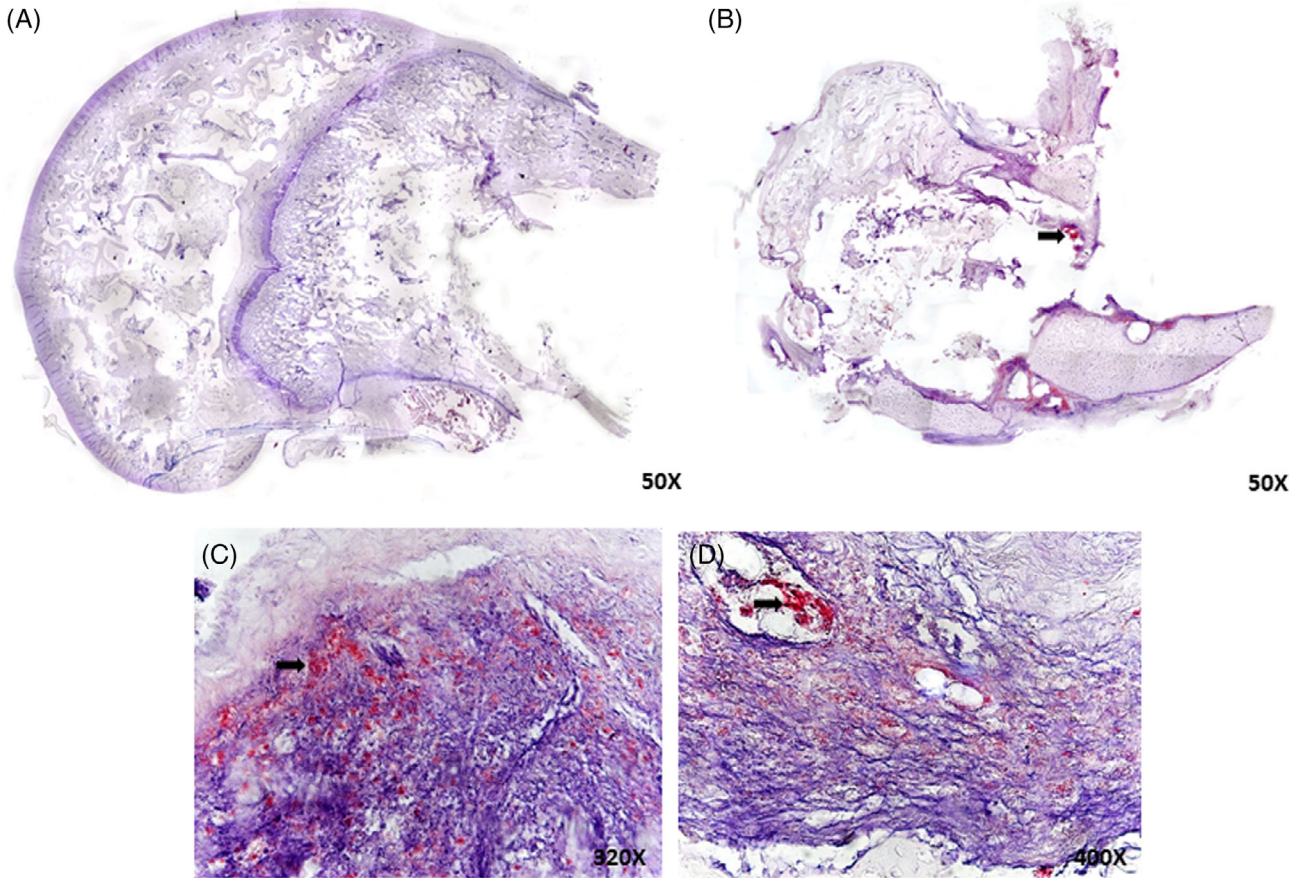


FIGURE 7. A: Panoramic view of RAM-11 IHC, sterile rod (50×). B: Panoramic view of RAM-11 IHC, contaminated rod (50×). C: RAM-11 IHC detail showing the contaminated rod + PLGA (320×). D: RAM-11 IHC detail showing the contaminated rod + PLGA (400×). Arrow indicates macrophage cells.

(micro-CT). These studies are based on experimental studies in animals and uninfected bone tissue. Perhaps the changes produced after a prosthetic infection may be defined using this technique in the future, but currently, this use is not possible today.

The investigation and improvement in the diagnosis and treatment of prosthetic infection relies on experimental

models of osteomyelitis, which must simulate the infection to properly examine and stage the bone repairing response. There is also no consensus on this point. Most studies¹¹ base their histological analysis on two classical scales, Smeltzer and Petty. The Smeltzer scale uses specific parameters of bone remodeling, such as periosteal reaction, acute and chronic inflammatory response, or the presence of necrosis.^{14,35} However, the assessment of the Smeltzer parameters is not always easy, especially if one is not an expert observer, because comparison of the bone response to a bacterial infection in an individualized manner produces a high percentage of variability in the affected bone areas.

A less used, but more useful scale from the histological point of view, is the Petty scale,¹⁵ which clearly describes the alterations that may occur in different bone structures: periosteum, cortex, and medullary canal. However, this model does not consider the reactive and reparative processes at the time of the study because it primarily takes into account the presence of inflammatory and immune cells and abscesses (corresponding all to processes of acute inflammation).

More recent studies expanded some parameters of the Smeltzer scale²² and combined or assessed both classic scales.¹⁶ These studies add new parameters to the classic inflammation and necrosis parameters, such as the formation of fibrosis and granular tissue. Others publications²³ also investigate more than one study time point and evaluate the

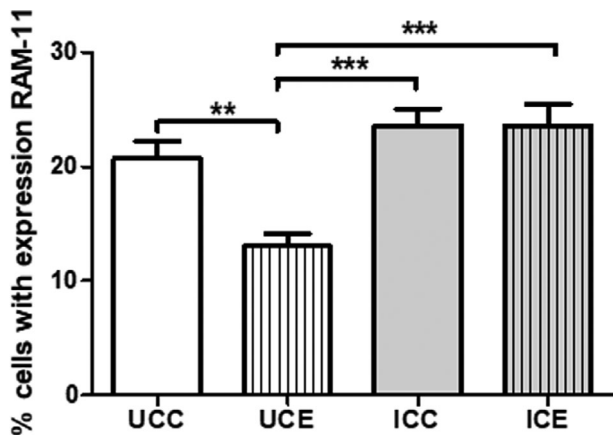


FIGURE 8. RAM-11 IHC percentage of positive expression. The macrophage response in groups with no infection was significantly higher in group 1 than group 2 ($p < 0.01$), while an adequate and similar macrophage response was observed in the contaminated groups. $**p < 0.01$, $***p < 0.001$.

response of bone tissue in an acute and chronic manner. However, all these studies have similar limitations to previous studies because the subjectivity and experience of the observer is essential, and the histological images presented are complex to interpret or, in some cases, even absent.

In this experimental model, a new histological scale is assessed for the parameters previously mentioned and for the preservation and remodeling of bone and cartilage histoarchitecture. Evaluation of the tissue in a global manner provides an overview of the capacity of bone repair and allows us to correlate the damage generated with the functionality of the tissue. The structure of the scale makes it useful for less experienced evaluators who may visualize the changes in the tissue in a clear and simple manner. This staging may be used in experimental models to evaluate any type of bone defect, even studies of uninfected biomaterials, which is possible only if the defect is examined with the surrounding new bone in a global view. Our model allows a detailed evaluation of the most reactive areas of tissue using the scales previously described in the literature, such as the number of cells, encapsulation of biomaterials, or new bone formation. The obtained results showed in a panoramic view the effects about the implanted rods, both sterile and contaminated and with commercial cements or modified with PLGA microspheres. This method allowed to obtain an easy perception of the general condition of the affected area due to the presence of the implant and the response obtained after 3 weeks. At the same time, we perform other cellular determinations. Among them, the macrophage response studied also suggests a less aggressive response in the groups that included PLGA, even in animals with infection. This combination of cements with PLGA showed great changes in contact with eroded bone, especially on infected bone. The preservation of bone structures and the increase of bone neof ormation were significantly improved. This modification in Palacos[®] cement may also be used to investigate the release of different antibiotics, which has already showed good results on *in vitro* studies.²¹

Therefore, there is no current unified definition or gold standard for the diagnosis and staging of osteomyelitis in animal models, and the establishment of a histological protocol to evaluate normal and pathological bones and the different phases of remodeling after an injury in a global manner remains a challenge. This article takes one step in this path and proposes a new method to stage the degree of bone destruction caused by infection in an experimental model. This proposal provides an approach about the possible effects after some necessary bone devices introduction in contact with infected bone areas. The histoarchitectural alterations will be the guide to understand the possible staging of the bone affectation and response. These new tools for a better diagnosis will lead to more appropriate treatment of patients affected by low-grade prosthetic infections.

CONFLICTS OF INTEREST STATEMENT

None declared.

REFERENCES

1. Maradit Kremers H, Larson D, Crowson C, Kremers W, Washington R, Steiner CA, Jiranek WA, Berry DJ. Prevalence of total hip and knee replacement in the United States. *J Bone Joint Surg Am* 2015;97(17):1386–1397.
2. Kurtz S, Ong K, Lau E, Bozic K. Impact of the economic downturn on total joint replacement demand in the United States. *J Bone Joint Surg Am* 2014;96(8):624–630.
3. Patel A, Pavlou G, Mújica-Mota RE, Toms AD. The epidemiology of revision total knee and hip arthroplasty in England and Wales: A comparative analysis with projections for the United States. A study using the National Joint Registry dataset. *Bone Joint J* 2015;97-B(8):1076–1081.
4. Allepuza A, Serra-Suttona V, Espallarguesa M, Sarriab A. Hip and knee replacement in the Spanish National Health System. *Rev Esp Cir Ortop Traumatol* 2009;53:290–299.
5. Berry DJ. Joint registries: What can we learn in 2016? *Bone Joint J* 2017;99-B(1 Suppl A):3–7.
6. Kurtz SM, Ong KL, Schmier J, Mowat F, Saleh K, Dybvik E, Kärrholm J, Garellick G, Havelin LI, Furnes O, Malchau H, Lau E. Future clinical and economic impact of revision total hip and knee arthroplasty. *J Bone Joint Surg Am* 2007;89(suppl 3):144–151.
7. Richard Lorio MD. Orthopaedic surgeon workforce and volume assessment for total hip and knee replacement in the United States: Preparing for an epidemic. *J Bone Joint Surg Am* 2008;90:1598–1605.
8. Esposito S, Leone S. Prosthetic joint infections: Microbiology, diagnosis, management and prevention. *Int J Antimicrob Agents* 2008; 32(4):287–293.
9. Jørgensen NP, Meyer RL, Dagnæs-Hansen F, Fuursted K, Petersen E. A modified chronic infection model for testing treatment of *Staphylococcus aureus* biofilms on implants. *PLoS One* 2014;9(10): e103688.
10. Nishitani K, Sutipornpalangkul W, de Mesy Bentley KL, Varrone JJ, Bello-Irizarry SN, Ito H, Matsuda S, Kates SL, Daiss JL, Schwarz EM. Quantifying the natural history of biofilm formation *in vivo* during the establishment of chronic implant-associated *Staphylococcus aureus* osteomyelitis in mice to identify critical pathogen and host factors. *J Orthop Res* 2015;33(9):1311–1319.
11. Reizner W, Hunter JG, NT O'M, Southgate RD, Schwarz EM, Kates SL. A systematic review of animal models for *Staphylococcus aureus* osteomyelitis. *Eur Cell Mater* 2014;27:196–212.
12. Jiang J, Li Y, Fang T, Zhou J, Li X, Wang YC, Dong J. Vancomycin-loaded nano-hydroxyapatite pellets to treat MRSA-induced chronic osteomyelitis with bone defect in rabbits. *Inflamm Res* 2011;61(3): 207–215.
13. Ding H, Zhao C, Cui X, Gu Y, Jia W, Rahaman MN, Wang Y, Huang WH, Zhang CQ. A novel injectable borate bioactive glass cement as an antibiotic delivery vehicle for treating osteomyelitis. *PLoS One* 2014;9(1):e85472.
14. Smeltzer M, Thomas J, Hickraon S, Skinner R, Nelson C, Griffith D, Parr TR Jr, Evans RP. Characterization of a rabbit model of staphylococcal osteomyelitis. *J Orthop Res* 1997;15(3):414–421.
15. Petty W, Spanier S, Shuster J, Silverthorne C. The influence of skeletal implants on incidence of infection. Experiments in a canine model. *J Bone Joint Surg* 1985;67(8):1236–1244.
16. Brooks B, Sinclair K, Grainger D, Brooks A. A resorbable antibiotic-eluting polymer composite bone void filler for perioperative infection prevention in a rabbit radial defect model. *PLoS One* 2015;10(3): e0118696.
17. Cui Q, Mihalko W, Shields J, Ries M, Saleh K. Antibiotic-impregnated cement spacers for the treatment of infection associated with total hip or knee arthroplasty. *J Bone Joint Surg Am* 2007;89(4):871–882.
18. Stevens C, Tetsworth K, Calhoun J, Mader J. An articulated antibiotic spacer used for infected total knee arthroplasty: A comparative *in vitro* elution study of simplex[®] and Palacos[®] bone cements. *J Orthop Res* 2005;23(1):27–33.
19. Anagnostakos K, Fürst O, Kelm J. Antibiotic-impregnated PMMA hip spacers: Current status. *Acta Orthop* 2006;77:628–637.
20. Anagnostakos K, Kelm J. Enhancement of antibiotic elution from acrylic bone cement. *J Biomed Mater Res Part B Appl Biomater* 2009;90 B:467–475.
21. Parra-Ruiz F, González-Gómez A, Fernández-Gutiérrez M, Parra J, García-García J, Azuara G, De la Torre B, Buján J, Ibarra B,

- Duocastella-Codina L, Molina-Crisol M, Vázquez-Lasa B, San Román J. Development of advanced biantibiotic loaded bone cement spacers for arthroplasty associated infections. *Int J Pharm* 2017;522(1–2):11–20.
22. Beenken K, Bradney L, Bellamy W, Skinner R, McLaren S, Gruenwald MJ, Spencer HJ, Smith JK, Haggard WO, Smeltzer MS. Use of xylitol to enhance the therapeutic efficacy of polymethylmethacrylate-based antibiotic therapy in treatment of chronic osteomyelitis. *Antimicrob Agents Chemother* 2012;56(11):5839–5844.
 23. Mistry S, Roy S, Maitra N, Kundu B, Chanda A, Datta S, Joy M. A novel, multi-barrier, drug eluting calcium sulfate/biphasic calcium phosphate biodegradable composite bone cement for treatment of experimental MRSA osteomyelitis in rabbit model. *J Control Release* 2016;239:169–181.
 24. Helbig L, Simank H, Lorenz H, Putz C, Wöfl C, Suda AJ, Moghaddam A, Schmidmaier G, Guehring T. Establishment of a new methicillin resistant *Staphylococcus aureus* animal model of osteomyelitis. *Int Orthop* 2013;38(4):891–897.
 25. Cazanave C, Greenwood-Quaintance K, Hanssen A, Karau M, Schmidt S, Gomez Urena EO, Mandrekar JN, Osmon DR, Lough LE, Pritt BS, Steckelberg JM, Patel R. Rapid molecular microbiologic diagnosis of prosthetic joint infection. *J Clin Microbiol* 2013;51(7):2280–2287.
 26. Ali F, Wilkinson J, Cooper J, Kerry R, Hamer A, Norman P, Stockley J. Accuracy of joint aspiration for the preoperative diagnosis of infection in total hip arthroplasty. *J Arthroplast* 2006;21(2):221–226.
 27. Font-Vizcarra L, García S, Martínez-Pastor J, Sierra J, Soriano A. Blood culture flasks for culturing synovial fluid in prosthetic joint infections. *Clin Orthop Relat Res* 2010;468(8):2238–2243.
 28. Van den Bekerom MP, Stuyck J. The value of pre-operative aspiration in the diagnosis of an infected prosthetic knee: A retrospective study and review of literature. *Acta Orthop Belg* 2006;72(4):441–447.
 29. Schäfer P, Fink B, Sandow D, Margull A, Berger I, Frommelt L. Prolonged bacterial culture to identify late periprosthetic joint infection: A promising strategy. *Clin Infect Dis* 2008;47(11):1403–1409.
 30. Vanhegan I, Morgan-Jones R, Barrett D, Haddad F. Developing a strategy to treat established infection in total knee replacement: A review of the latest evidence and clinical practice. *Bone Joint J* 2012;94-B(7):875–881.
 31. Meermans G, Haddad F. Is there a role for tissue biopsy in the diagnosis of periprosthetic infection? *Clin Orthop Relat Res* 2010;468(5):1410–1417.
 32. Corona P, Gil E, Guerra E, Soldado F, Amat C, Flores X, Pigrau C. Percutaneous interface biopsy in dry-aspiration cases of chronic periprosthetic joint infections: A technique for preoperative isolation of the infecting organism. *Int Orthop* 2011;36(6):1281–1286.
 33. Martínez-Perez M, Pérez-Jorge C, Lozano D, Portal-Nuñez S, Pérez-Tanoira R, Conde A, Arenas MA, Hernández-López JM, de Damborenea JJ, Gomez-Barrena E, Esbrit P, Esteban J. Evaluation of bacterial adherence of clinical isolates of *Staphylococcus* sp. using a competitive model. *Bone Joint Res* 2017;6(5):315–322.
 34. Li Z, Kuhn G, Von Salis-Sogli M, Cooke S, Schirmer M, Müller R, Ruffoni D. *In vivo* monitoring of bone architecture and remodeling after implant insertion: The different responses of cortical and trabecular bone. *Bone* 2015;81:468–477.
 35. Gillaspay AF, Hickmon SG, Skinner RA, Thomas JR, Nelson CL, Smeltzer MS. Role of the accessory gene regulator (*agr*) in pathogenesis of staphylococcal osteomyelitis. *Infect Immun* 1995;63(9):3373–3380.